Chaos in A Spacecraft Passive Attitude Maneuver and the Marsden Energy Sink

A nice report!
jm.

MA 189
Fall 1993
Project Report

Charles P. Coleman
charles@robotics.eecs.berkeley.edu
(510) 643-5806

Department of Electrical Engineering and Computer Sciences
University of California at Berkeley
Berkeley, CA 94720 USA

December 13, 1993

Abstract

This report contains a review and explication of the paper "Chaos in a Spacecraft Passive Attitude Maneuver Due to Time-Periodic Perturbations", by G. L. Gray, I. Dobson, and D. C. Kammer [Gray, Dobson and Kammer 92].

The report also contains contains an analysis of the energy sink proposed by J. E. Marsden, and a comparison of the Marsden energy sink with the [Kammer and Gray 92] energy sink.

Contents

1 Introduction

The first part of this report consists of a review and explication of the paper "Chaos in a Spacecraft Passive Attitude Maneuver Due to Time-Periodic Perturbations", by G. L. Gray, I. Dobson, and D. C. Kammer [Gray, Dobson and Kammer 92].

The second part of this report contains an analysis of the energy sink proposed by J. E. Marsden, and a comparison of the Marsden energy sink with the [Kammer and Gray 92] energy sink.

2 Outline of the Report

2.1 Overview of [Gray, Dobson and Kammer 92]

Section 3 contains a brief description of the analysis and results given in [Gray, Dobson and Kammer 92].

2.2 A Closer Look at [Gray, Dobson and Kammer 92]

Sections 4 through 15 provide a more detailed description of the analysis and results of [Gray, Dobson and Kammer 92]. These sections present the key elements of the mathematical analysis presented in [Gray, Dobson and Kammer 92].

2.3 Presenting and Comparing the Marsden Energy Sink

Section 16 presents the Marsden energy sink. Section 17 compares the Marsden energy sink with the [Kammer and Gray 92] energy sink.

3 Overview of [Gray, Dobson and Kammer 92]

3.1 Dynamics of a Rotating Quasi-Rigid Body with Oscillating Sub-Bodies

In [Gray, Dobson and Kammer 92], the authors use Melnikov's method to study the chaotic dynamics of a passive attitude transition maneuver of a model satellite.

The model satellite consists of a quasi-rigid carrier body containing two small masses which oscillate along the minimum principal axis of inertia of the carrier body.

The satellite is torque-free and is going from minor axis spin to major axis spin, under the influence of small kinetic energy damping, and under the influence of the oscillation of the two small sub-bodies.

3.2 Quasi-Rigidity

When a quasi-rigid body is not spinning about a principal axis, it is assumed that internal body motions occur which cause kinetic energy to be dissipated. This effect is called *damping*, as the kinetic energy is damped during these motions.

When a quasi-rigid body is spinning about one of its principal axes, it becomes rigid. No internal motions occur and no kinetic energy is dissipated.

Note that since the quasi-rigid body is torque free, the magnitude of the angular momentum vector is preserved for all rotational motions.

3.3 Computationally Simulating Quasi-Rigidity with Energy Sinks

It is assumed that internal motions, when they occur, are governed by the elastic constituency relations of the body. These relations, however, are not modeled for computational purposes. Instead, a seemingly arbitrary computational factor which

- dissipates kinetic energy for non-principal axis rotations
- and preserves the magnitude of the angular momentum vector

is added to the rigid body equations of motion of the body. These computational factors are called *energy sinks.*

There may be quite a large family of such computational factors which dissipate kinetic energy for non-principal axis rotations, and preserve the magnitude of the angular momentum vector. In fact, J. E. Marsden has presented one other such computation factor which satisfies these conditions. This computational factor will be presented in Section 16.

3.4 Chaos

[Gray, Dobson and Kammer 92] show that chaotic motion can be caused by the oscillation of modeled small sub-bodies inside the satellite during a minor axis spin to major axis spin passive attitude maneuver. This chaotic motion is due to the formation of Smale horseshoes. Melnikov's method is used to analytically detect chaos.

It is suggested that the model satellite is a reasonable engineering model, which demonstrates that it is possible for chaotic motion to occur in a similar passive attitude maneuver for actual spacecraft.

3.5 Using Melnikov's Method to Detect Chaos

In order to use Melnikov's method, an improper integral has to be calculated. A great deal of the analytical effort performed by [Gray, Dobson and Kammer 92], involves transforming the equations of motion of the model satellite into a form so that the required improper integral can be calculated.

3.6 Conclusions - Analytic Criterion for Chaos

[Gray, Dobson and Kammer 92] show that the Melnikov function computed for the model satellite has simple zeros, indicating the existence of chaos of sufficiently small ϵ. The zeros are written as a function of standard spacecraft system parameters.

[Gray, Dobson and Kammer 92] conclude by presenting several discussion on the effect of model satellite parameters on the formation of chaos. They conclude with brief satement of satellite design criteria which will avoid chaos in a passive minor axis to major axis spin attitude maneuver.

4 Model Satellite

4.1 Quasi-Rigid Carrier Body with Two Small Oscillating Sub-Bodies

The model satellite consists of a quasi-rigid carrier body which contains two small oscillating masses.

4.2 Model Satellite Configuration

The configuration of the model satellite given in [Gray, Dobson and Kammer 92] is given in Figure 1.

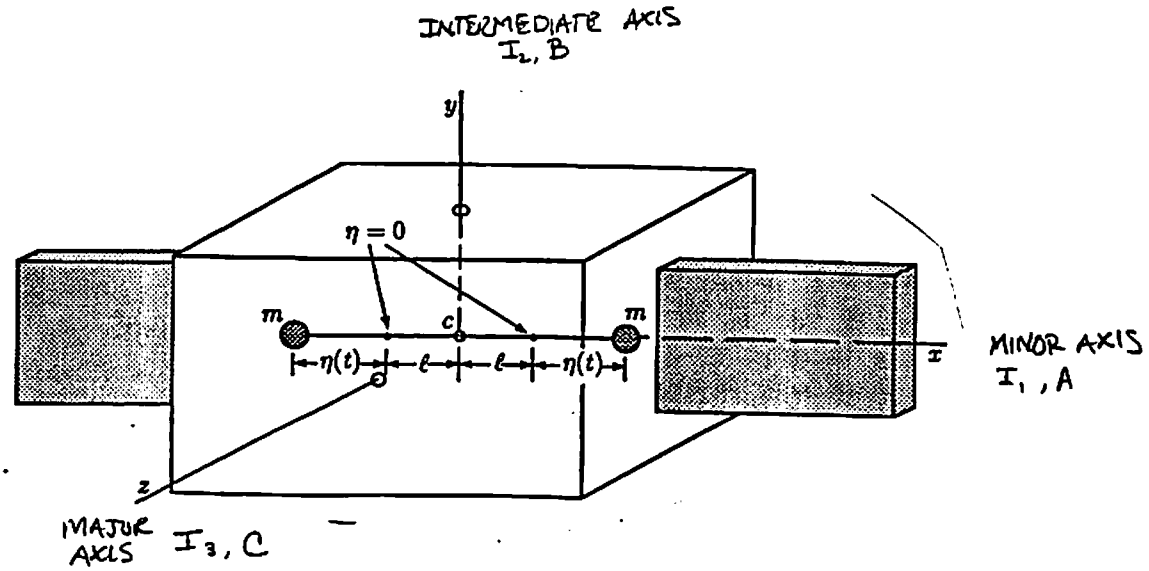

Figure 1: Model Satellite

4.3 Carrier Body

The mass center of the carrier body is denoted by c. A body-fixed orthogonal coordinate system is aligned with the principal axes of the carrier body and centered at c, and is denoted by x, y, z.

The principal moments of inertia for the carrier body are designated I_1, I_2, I_3. The carrier body principal moments of inertia are assumed distinct, and it is assumed that $I_1 < I_2 < I_3$.

The x-axis is the minor axis of rotation for the carrier body and for the complete satellite. The y-axis is the intermediate axis of rotation for the carrier body and for the complete satellite. The z-axis is the major axis of rotation for the carrier body and the complete satellite.

4.4 Sub-Body Locations - $\eta(t)$

The two sub-bodies oscillate symmetrically with respect to c along the x-axis. Hence, the satellite's mass center c does not move relative to the carrier body.

The position of the sub-bodies relative to the main body is a *known* periodic function of time, and is denoted by $\eta(t)$.

The $\eta = 0$ position is located a distance l from the mass center c. $\eta(t)$ is restricted so that the motion of the two masses does not pass through the satellite's mass center c. For this analysis $\eta(t)$ is given by

$$\eta(t) = \eta_0 \cos(\Omega t)$$

4.5 Carrier Body Principal Moments of Inertia

The inertia tensor for the carrier body alone, without sub-bodies is

$$\begin{bmatrix} I_1 & 0 & 0 \\ 0 & I_2 & 0 \\ 0 & 0 & I_3 \end{bmatrix}$$

4.6 Reference Configuration Principal Moments of Inertia

The small sub-bodies, essentially point masses, have no affect on the principal moment of inertia about the x-axis. They do, however, by the parallel axis theorem, add terms to the principal moments of inertia bout the y and z-axes.

The inertia tensor for carrier body and sub-bodies, and for $\eta(t) \equiv 0$ is

$$\begin{bmatrix} I_1 & 0 & 0 \\ 0 & I_2 + 2ml^2 & 0 \\ 0 & 0 & I_3 + 2ml^2 \end{bmatrix}$$

This will be taken as the reference configuration of the satellite.

It is common within the aerospace engineering literature to denote the principal moments of inertia of a satellite about an x, y, z-coordinate system located at a satellite's mass center, by A, B, and C, respectively.

Using aerospace engineering nomenclature, define the following quatities for the reference configuration inertia tensor

$$\begin{aligned} A &= I_1 \\ B &= I_2 + 2ml^2 \\ C &= I_3 + 2ml^2 \end{aligned}$$

4.7 Satellite Principal Moments of Inertia

The inertia tensor for the carrier body and sub-bodies, and arbitrary η is given by

$$\begin{bmatrix} I_1 & 0 & 0 \\ 0 & I_2 + 2m(l+\eta(t))^2 & 0 \\ 0 & 0 & I_3 + 2m(l+\eta(t))^2 \end{bmatrix}$$

Setting

$$\Delta = 2m(2l\eta(t) + \eta(t)^2)$$

The inertia tensor for the carrier body and sub-bodies, with movement of the sub-bodies given by $\eta(t)$ is given by

$$\begin{bmatrix} A & 0 & 0 \\ 0 & B+\Delta & 0 \\ 0 & 0 & C+\Delta \end{bmatrix}$$

Since $\eta(t) = \eta_0 \cos(\Omega t)$ is known as a function of time, the satellite inertia tensor is known as a function of time, and it can be used in calculations for the equations of motion of the satellite.

4.8 Sub-Body Inertia Tensor Effects

Note that the inertia tensor perturbations produced by the oscillating sub-bodies do not produce cross-product moment of inertia terms.

4.9 Restrictions on Mass and Motion of Sub-bodies

It is assumed that the inertia tensor perturbations caused by the oscillating sub-bodies is small. This assumption is necessary in order to apply Melnikov's method.

When the equations of motion of the model satellite are non-dimensionalized, the effect of the oscillating sub-bodies will be described with respect to a perturbation parameter ϵ. The motion of the sub-bodies will then be assumed to have an $O(\epsilon)$ perturbing effect on the spacecraft.

5 Undamped Equations of Motion

The system of differential equations describing the motion of the *undamped* (non-energy dissipating) model satellite, in terms of principal *body angular momentum* components is given below.

This report retains the aerospace engineering convention for denoting the principal moments of inertia as used in [Gray, Dobson and Kammer 92], but convert the body angular momentum components to notation, Π_1, Π_2, and Π_3 used in [Marsden and Ratiu 93].

$$\begin{aligned}
\dot{\Pi}_1 &= \left[\frac{B-C}{(B+\Delta)(C+\Delta)}\right]\Pi_2\Pi_3 \\
\dot{\Pi}_2 &= \left[\frac{(C+\Delta)-A}{(C+\Delta)A}\right]\Pi_3\Pi_1 \\
\dot{\Pi}_3 &= \left[\frac{A-(B+\Delta)}{A(B+\Delta)}\right]\Pi_1\Pi_2
\end{aligned}$$

6 Quantifying Energy Damping Effects

6.1 Energy Sinks

Damping terms which dissipate kinetic energy for non-principal axis rotations, and which preserve the magnitude of the angular momentum vector, are added to the undamped equations of motion. These damping terms are collectively called an energy sink.

6.2 [Kammer and Gray 92] Energy Sink

The [Kammer and Gray 92] energy sink is used in [Gray, Dobson and Kammer 92]. The [Kammer and Gray 92] energy sink has the form

$$\begin{bmatrix} u_1 \\ u_2 \\ u_3 \end{bmatrix} = \beta \begin{bmatrix} -\Pi_1\Pi_2^2 \\ \Pi_1^2\Pi_2 - \Pi_2\Pi_3^2 \\ \Pi_2^2\Pi_3 \end{bmatrix}$$

In [Kammer and Gray 92], this energy sink is known to dissipate kinetic energy for non-principal axis rotations, and preserve the magnitude of the angular momentum vector.

The proof will not be repeated in this report, but can be found in [Kammer and Gray 92, pp 55-56, Eqns (1), (2), and (7)]. The authors do not present the inspiration for their energy sink in [Kammer and Gray 92].

6.3 Adding the Energy Sink Terms to the Equations of Motion

The [Kammer and Gray 92] energy sink is added to equations of motion to quantitatively simulate the kinetic energy dissipation which occurs in rotational motion for quasi-rigid

bodies. With the [Kammer and Gray 92] energy sink terms, the equations of motion for the model satellite become

$$\begin{aligned}
\dot{\Pi}_1 &= \left[\frac{B-C}{(B+\Delta)(C+\Delta)}\right]\Pi_2\Pi_3 + u_1 \\
\dot{\Pi}_2 &= \left[\frac{(C+\Delta)-A}{(C+\Delta)A}\right]\Pi_3\Pi_1 + u_2 \\
\dot{\Pi}_3 &= \left[\frac{A-(B+\Delta)}{A(B+\Delta)}\right]\Pi_1\Pi_2 + u_3
\end{aligned}$$

6.4 Restrictions on Kinetic Energy Dissipation

It is assumed that the kinetic energy dissipation provided by the energy sink is small. This assumption is necessary in order to apply Melnikov's method.

When the equations of motion of the model satellite are non-dimensionalized, the energy dissipation terms will be described with respect to a perturbation parameter ϵ. The energy sink will then be assumed to have an $O(\epsilon)$ effect on the equations of motion of the spacecraft.

7 Perturbed Equations of Motion

Writing out the terms for the [Kammer and Gray 92] energy sink explicitly in terms of the components of the body angular momentum, the equations of motion of the model satellite become

$$\begin{aligned}
\dot{\Pi}_1 &= \left[\frac{B-C}{(B+\Delta)(C+\Delta)}\right]\Pi_2\Pi_3 - \beta\Pi_1\Pi_2^2 \\
\dot{\Pi}_2 &= \left[\frac{(C+\Delta)-A}{(C+\Delta)A}\right]\Pi_3\Pi_1 + \beta(\Pi_1^2\Pi_2 - \Pi_2\Pi_3^2) \\
\dot{\Pi}_3 &= \left[\frac{A-(B+\Delta)}{A(B+\Delta)}\right]\Pi_1\Pi_2 + \beta\Pi_2^2\Pi_3
\end{aligned}$$

Note that these added terms are cubic in the components of the body angular momentum.

8 Unperturbed Equations of Motion

The unperturbed equations of motion are the equations of motion for the non-energy dissipating reference configuration satellite. They are given below.

$$\dot{\Pi}_1 = \left[\frac{B-C}{BC}\right]\Pi_2\Pi_3$$

$$\dot{\Pi}_2 = \left[\frac{C-A}{CA}\right]\Pi_3\Pi_1$$
$$\dot{\Pi}_3 = \left[\frac{A-B}{AB}\right]\Pi_1\Pi_2$$

9 Nondimensionalizing the Equations of Motion

The equations of motion of the model satellite, a quasi-rigid carrier body with two small oscillating sub bodies, are nondimensionalized so that all resulting quantities except ϵ are $O(1)$.

9.1 Nondimensional Principal Moments of Inertia

The principal moment of inertia about the intermediate axis, B, is used to nondimensionalize the three principal moments of inertia.

It is assumed that

$$0 < A < B < C$$

Dividing by B this inequality becomes

$$0 < \frac{A}{B} < 1 < \frac{C}{B}$$

Defining

$$r_2 = \frac{A}{B} \qquad r_1 = \frac{C}{B}$$

we have

$$0 < r_1 < 1 < r_2$$

The inequality

$$C < A + B$$

also holds.

Dividing by B and using the definitions of r_1 and r_2 this inequality becomes

$$r_1 < 1 + r_2$$

Combining the two inequalities results in the statement

$$0 < r_2 < 1 < r_1 < 1 + r_2 < 2$$

9.2 Definition of ϵ

Since the principal moment of inertia about the intermediate axis, B, is used to nondimensionalize the three principal moments of inertia, it is also used to define ϵ, the perturbation parameter.

The perturbation parameter ϵ is given by

$$\epsilon = \frac{ml^2}{B}$$

So for ϵ to be small, it is required that $ml^2 << B$.

9.3 Other Nondimensional Quantities

Letting $||\Pi|| = H \in \mathbf{R}$ represent the total angular momentum, and using B and ml^2 several other nondimensional quantities are defined.

9.4 Nondimensional Time τ

Nondimensional time τ, is defined as

$$\tau = \frac{Ht}{B}$$

Differentiation with respect to nondimensional time is given by

$$()' = \frac{d}{d\tau}()$$

9.5 Nondimensional Body Angular Momentum Components

The nondimensional body angular momentum components and their time derivatives are given by

$$\tilde{\Pi}_i = \frac{\Pi_i}{H}$$

$$\tilde{\Pi}_i' = \frac{B}{H^2}\dot{\Pi}_i$$

Note that the magnitude of the nondimensionalize body angular momentum vector is 1.

$$||\tilde{\Pi}|| = \sqrt{\tilde{\Pi}_1^2 + \tilde{\Pi}_2^2 + \tilde{\Pi}_3^2} = 1$$

9.6 Nondimensional Δ and β

The effect of the oscillating sub-bodies, given by Δ, and the effect of energy dissipation, whose magnitude is quantified by β, are nondimensionalized as follows

$$\tilde{\Delta} = \frac{\Delta}{\epsilon B}$$

$$\tilde{\beta} = \beta\frac{HB^2}{ml^2}$$

9.7 Nondimensional Form of $\eta(t)$

The nondimensional time-dependent form of η is formulated by defining the following quantities

$$\tilde{\eta} = \frac{\eta}{l}$$

$$\tilde{\Omega} = \frac{\Omega B}{H}$$

With these definitions $\eta(t) = \eta_0 \cos(\Omega t)$ is nondimensionalized and becomes

$$\tilde{\eta}(t) = \frac{\eta_0}{l} \cos(\tilde{\Omega}\tau)$$

10 Nondimensional Perturbed Equations of Motion

Using the quantities defined in the previous sections, the non-dimensionalized equations of motion for the model satellite are

$$\begin{aligned}
\tilde{\Pi}_1' &= \left[\frac{1 - r_1}{(1 + \epsilon\tilde{\Delta})r_1 + \epsilon\tilde{\Delta})}\right] \tilde{\Pi}_2\tilde{\Pi}_3 - \epsilon\tilde{\beta}\tilde{\Pi}_1\tilde{\Pi}_2^2 \\
\tilde{\Pi}_2' &= \left[\frac{(r_1 + \epsilon\tilde{\Delta}) - r_2}{(r_1 + \epsilon\tilde{\Delta})r_2}\right] \tilde{\Pi}_3\tilde{\Pi}_1 + \epsilon\tilde{\beta}(\tilde{\Pi}_1^2\tilde{\Pi}_2 - \tilde{\Pi}_2\tilde{\Pi}_3^2) \\
\tilde{\Pi}_3' &= \left[\frac{r_2 - (1 + \epsilon\tilde{\Delta})}{(1 + \epsilon\tilde{\Delta})r_2}\right] \tilde{\Pi}_1\tilde{\Pi}_2 + \epsilon\tilde{\beta}\tilde{\Pi}_2^2\tilde{\Pi}_3
\end{aligned}$$

10.1 Order $O(\epsilon)$ Effects

It is clear from the structure of the nondimensionalized equations of motion, that the effects of oscillating sub-bodies and of the energy sink have been recast so that they have an $O(\epsilon)$ effect.

10.2 The Perturbed Phase Space

The attitude dynamics of the model satellite occur on the surface of the angular momentum sphere. These dynamics are depicted in Figure 2.

11 Nondimensional Unperturbed Equations of Motion

When $\epsilon = 0$ we recover the nondimensionalized equations of motion for the non-energy dissipating reference configuration model satellite.

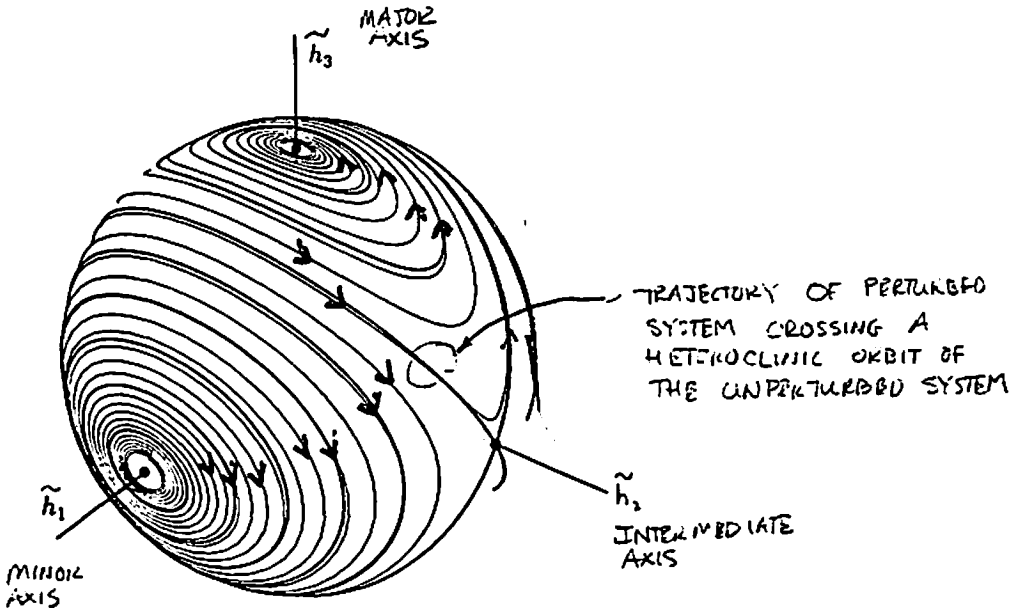

Figure 2: Perturbed Dynamics

$$\begin{aligned}
\tilde{\Pi}_1' &= \left[\frac{1-r_1}{r_1}\right]\tilde{\Pi}_2\tilde{\Pi}_3 \\
\tilde{\Pi}_2' &= \left[\frac{r_1-r_2}{r_1 r_2}\right]\tilde{\Pi}_3\tilde{\Pi}_1 \\
\tilde{\Pi}_3' &= \left[\frac{r_2-1}{r_2}\right]\tilde{\Pi}_1\tilde{\Pi}_2
\end{aligned}$$

11.1 The Unperturbed Phase Space

The attitude dynamics of the reference configuration satellite occur on the surface of the angular momentum sphere. These dynamics are depicted in Figure 3

11.2 The Angular Momentum Sphere

The angular momentum sphere possesses six equilibria corresponding to positive and negative spin about each of the three principal axes of the unperturbed non-energy dissipating satellite. Two of the equilibria, corresponding to spin about the intermediate principal axis, are saddles.

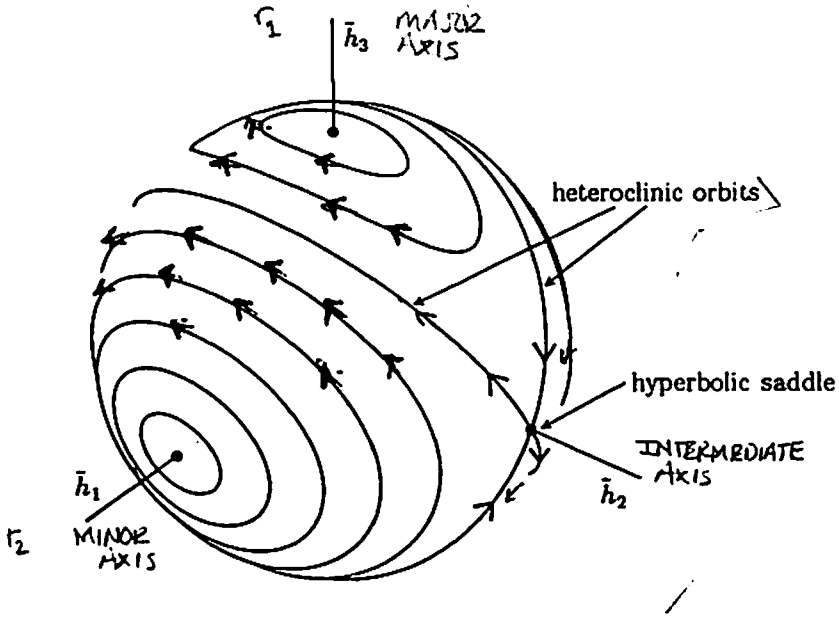

Figure 3: Unperturbed Dynamics

11.3 Heteroclinic Orbits

There are four heteroclinic orbits linking the angular momentum sphere's two saddles. In a passive attitude transition from minor axis to major axis spin, the trajectory of the perturbed system must cross a heteroclinic orbit of the unperturbed system.

The equations for the heteroclinic orbits of the unperturbed system are

$$\bar{\Pi}_1 = \pm \left[\frac{r_2(1-r_1)}{r_2 - r1}\right]^{\frac{1}{2}} \operatorname{sech}\left\{\left[\frac{(r_2-1)(1-r_1)}{r_2 r1}\right]^{\frac{1}{2}} \tau\right\}$$

$$\bar{\Pi}_2 = \pm \tanh\left\{\left[\frac{(r_2-1)(1-r_1)}{r_2 r1}\right]^{\frac{1}{2}} \tau\right\}$$

$$\bar{\Pi}_3 = \pm \left[\frac{r_2(r_2-1)}{r_2 - r1}\right]^{\frac{1}{2}} \operatorname{sech}\left\{\left[\frac{(r_2-1)(1-r_1)}{r_2 r1}\right]^{\frac{1}{2}} \tau\right\}$$

Melnikov's method is used to study the chaotic motion in the perturbed system that may occur near the heteroclinic orbits of the unperturbed system.

12 Melnikov's Method

12.1 A Tool to Detect Chaos

Melnikov's method can be used to detect chaos in a system of differential equations such as those governing the model satellite.

Melnikov's method is a perturbation technique for proving the existence of transverse homoclinic orbits to hyperbolic periodic orbits in a class of time-periodic vector fields. The existence of transverse homoclinic orbits implies the existence of horseshoes and chaos via the Smale-Birkhoff Homoclinic Theorem.

12.2 Appropriate Systems

In the notation given in [Gray, Dobson and Kammer 92] Melnikov's method considers systems of the form

$$\dot{\mathbf{x}} = \mathbf{f}(\mathbf{x}) + \epsilon \mathbf{g}(\mathbf{x}, t) \qquad \mathbf{x} \in \mathbf{R}^2$$

where $\mathbf{g}$ is of period T in t, $\mathbf{f}(\mathbf{x})$ is a Hamiltonian vector field defined on $\mathbf{R}^2$ and $\epsilon \mathbf{g}(\mathbf{x}, t)$ is a small perturbation which in not necessarily Hamiltonian.

12.3 Restrictions on the Unperturbed System

Melnikov's method uses globally computable solutions of the unperturbed ($\epsilon = 0$) integrable system

$$\dot{\mathbf{x}} = \mathbf{f}(\mathbf{x})$$

to study the perturbed solution.

The unperturbed system is assumed to possess a homoclinic orbit to a hyperbolic saddle point. Denote this orbit by $\mathbf{q}_0(t)$.

12.4 Detecting Transverse Homoclinic Orbits

Melnikov's method determines whether or not transverse homoclinic points exist by searching for intersections of stable and unstable manifolds W^s and W^u of the hyperbolic saddle point. It does this by parameterizing the distance between W^s and W^u to $O(\epsilon)$.

The distance function is called the *Melnikov function.* It is is denoted by $M(t_0)$ and is defined as follows

$$M(t_0) = \int_{-\infty}^{\infty} \mathbf{f}(\mathbf{q}_0(t)) \wedge \mathbf{g}(\mathbf{q}_0(t), t + t_0)\, dt$$

where $\wedge$ is given by

$$\mathbf{a} \times \mathbf{b} = a_1 b_2 - a_2 b_1$$

and $t_0 \in [0, T]$.

If the Melnikov function does have simple zeros, then the W^s and W^u manifolds intersect transversally and the system is chaotic for sufficiently small ϵ.

The zeros of the Melnikov function indicate the values of the system parameters for which the system exhibits chaos.

12.5 Application to the Nondimensional Perturbed Equations of Motion

Melnikov's method applies equally well to systems with heteroclinic cycles. Since heteroclinic orbits exist in the phase space of the nondimensional unperturbed equations of motion, Melnikov's method can be applied to test for chaos in the nondimensional perturbed system.

13 Nondimensional Perturbed Equations of Motion to $O(\epsilon)$

Binomial expansions are used to write the nondimensional perturbed equations of motion to terms through $O(\epsilon)$. The resulting equations are

$$\begin{aligned}
\tilde{\Pi}_1' &= \left[\frac{1-r_1}{r_1}\right]\tilde{\Pi}_2\tilde{\Pi}_3 - \epsilon\left[\left(\frac{1-r_1^2}{r_1^2}\right)\tilde{\Delta}\tilde{\Pi}_2\tilde{\Pi}_3 + \tilde{\beta}\tilde{\Pi}_1\tilde{\Pi}_2^2\right] \\
\tilde{\Pi}_2' &= \left[\frac{r_1-r_2}{r_1 r_2}\right]\tilde{\Pi}_3\tilde{\Pi}_1 + \epsilon\left[\frac{\tilde{\Delta}}{r_1^2}\tilde{\Pi}_1\tilde{\Pi}_3 + \tilde{\beta}\tilde{\Pi}_2(\tilde{\Pi}_1^2 - \tilde{\Pi}_3^2)\right] \\
\tilde{\Pi}_3' &= \left[\frac{r_2-1}{r_2}\right]\tilde{\Pi}_1\tilde{\Pi}_2 + \epsilon\left[\tilde{\beta}\tilde{\Pi}_2^2\tilde{\Pi}_3 - \tilde{\Delta}\Pi_1\tilde{\Pi}_2\right]
\end{aligned}$$

14 Calculating the Melnikov Function

14.1 Spherical Coordinates

All of the information needed to calculate the Melnikov function is nearly available. The equations for the heteroclinic orbits $\mathbf{q}_0(t)$ of the unperturbed system are given in Section 11.3 in three dimensions. The perturbed system of differential equations

$$\dot{\mathbf{x}} = \mathbf{f}(\mathbf{x}) + \epsilon\mathbf{g}(\mathbf{x}, t)$$

is given in Section 13 in three dimensions. However, Melnikov method requires the heteroclinic orbit equations and perturbed system of equations to be two dimensions.

The angular momentum sphere is a two dimensional surface embedded in three dimensions. Making a change of variables from rectangular coordinates to spherical coordinates gives $\mathbf{q}_0(t)$ and $\dot{\mathbf{x}} = \mathbf{f}(\mathbf{x}) + \epsilon\mathbf{g}(\mathbf{x}, t)$ in in two dimensional form.

Up to this point, the algebraic manipulations of the equations of motion have been instructive. Transforming $\mathbf{q}_0(t)$ and $\dot{\mathbf{x}} = \mathbf{f}(\mathbf{x}) + \epsilon\mathbf{g}(\mathbf{x}, t)$ into spherical coordinates requires manual and computer manipulation. These calculations do not add to the exposition of [Gray, Dobson and Kammer 92] are not instructive and are not be presented.

14.2 Residue Theorem

Once the $\mathbf{q}_0(t)$ and $\dot{\mathbf{x}} = \mathbf{f}(\mathbf{x}) + \epsilon \mathbf{g}(\mathbf{x}, t)$ have been transformed, the wedge product under the Melnikov integral is computed. The Melnikov integral is then evaluated using the residue theorem of complex variable theory.

14.3 Simple Zeros

Simple zeros are found to exist for the calculated Melnikov function for the model satellite system. A complicated expression for the zeros as a function of system parameters is derived. Several plots are made to aid in the interpretation of the criterion for chaos.

14.4 Important System Parameters

The zeros of the Melnikov function are found to depend on five following system parameters. They are the

- Moment of Inertia Parameters r_1 and r_2
- Forcing Frequency $\tilde{\Omega}$
- Forcing Amplitude $\tilde{\eta}$
- and Damping $\tilde{\beta}$

By fixing two of the parameters, a three-dimensional plot of the surface separating chaotic from nonchaotic motion can be drawn as a function of the remaining three variables. Conclusions can be drawn about the effects of the values of the parameters of satellite system on the formation of chaos.

It is important to note that these results correspond *specifically* to the particular satellite model given in [Gray, Dobson and Kammer 92]. They are not necessarily general conclusions that can be stated for satellite dynamics.

Nonetheless, the construction of the concluding arguments presented in [Gray, Dobson and Kammer 92] is instructive. An representative example of the type of analysis of chaos in the [Gray, Dobson and Kammer 92] satellite system is given in the next section.

15 A Sample Effect of System Parameters On The Formation of Chaos

For $r_2 = \frac{2}{3}$, $\tilde{\beta} = 1$, the surface separating chaotic from nonchaotic motion is given in Figure 4. Values above the surface correspond to chaotic motion. Those below correspond to nonchaotic motion.

It is required that $\tilde{\eta} < 1$ so that the two masses do not pass through the satellite mass center c.

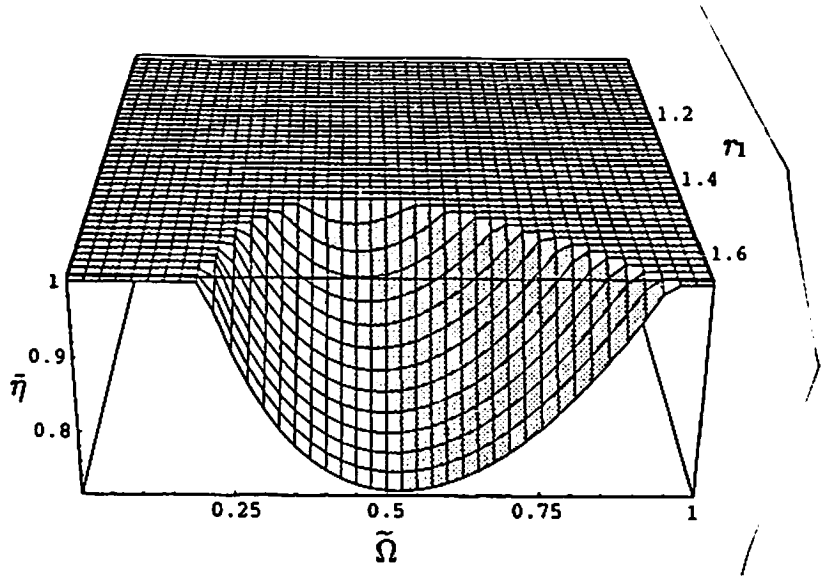

Figure 4: Separation Surface

The forcing frequency $\tilde{\Omega}$, the forcing amplitude $\bar{\eta}$, and the shape of the satellite r_2 can be varied, and their effects on the formation of chaos observed in Figure 4.

It is found that for small and large values of the forcing frequency $\tilde{\Omega}$, it is impossible to obtain chaos for any values of the forcing amplitude $\bar{\eta} < 1$. But for an intermediate values of $\tilde{\Omega}$ near .5, chaos is easier to attain and it is virtually assured for large values of the maximum moment of inertia r_2.

It is also found that for values of r_1 approaching unity, which corresponds to a nearly symmetric prolate rigid body, no chaotic motion occurs for the constant values of r_2 and $\tilde{\beta}$ chosen and for $\bar{\eta} < 1$, and for *any* value of $\tilde{\Omega}$.

16 Marsden Energy Sink

The equations of motion for a rigid body can be written as

$$\dot{\Pi} = \Pi \times \Omega$$

Defining

$$A_1 = \frac{I_2 - I_3}{I_2 I_3}$$

$$A_2 = \frac{I_3 - I_1}{I_1 I_3}$$

$$A_3 = \frac{I_1 - I_2}{I_1 I_2}$$

these equations become

$$\begin{bmatrix} \dot{\Pi}_1 \\ \dot{\Pi}_2 \\ \dot{\Pi}_3 \end{bmatrix} = \begin{bmatrix} A_1 \cdot \Pi_2 \Pi_3 \\ A_2 \cdot \Pi_1 \Pi_3 \\ A_3 \cdot \Pi_1 \Pi_2 \end{bmatrix}$$

16.1 Computational Terms

The energy sink proposed by Marsden is $\alpha\,\Pi \times (\Pi \times \Omega)$ where $\alpha > 0$. The rigid body equations of motion with terms added become

$$\dot{\Pi} = \Pi \times \Omega \; + \; \alpha\,\Pi \times (\Pi \times \Omega)$$

or

$$\begin{bmatrix} \dot{\Pi}_1 \\ \dot{\Pi}_2 \\ \dot{\Pi}_3 \end{bmatrix} = \begin{bmatrix} A_1 \cdot \Pi_2 \Pi_3 \\ A_2 \cdot \Pi_1 \Pi_3 \\ A_3 \cdot \Pi_1 \Pi_2 \end{bmatrix} + \begin{bmatrix} u_1' \\ u_2' \\ u_3' \end{bmatrix}$$

where

$$\begin{bmatrix} u_1' \\ u_2' \\ u_3' \end{bmatrix} = \alpha \begin{bmatrix} A_3 \cdot \Pi_1 \Pi_2^2 - A_2 \cdot \Pi_1 \Pi_3^2 \\ -A_3 \cdot \Pi_1^2 \Pi_2 + A_1 \cdot \Pi_2 \Pi_3^2 \\ A_2 \cdot \Pi_1^2 \Pi_3 - A_1 \cdot \Pi_2^2 \Pi_3 \end{bmatrix}$$

The Marsden energy sink is cubic in the components of the body angular momentum vector.

The Marsden energy sink preserves the magnitude of the angular momentum vector, and dissipates kinetic energy H for non-principal axis rotations as shown in the following two sections. The equation motion of the angular momentum vector in inertial space is presented in the third following section.

16.2 Preservation of the Magnitude of the Angular Momemtum Vector

• $\|\Pi\|^2$ is conserved

To show $\|\Pi\|^2$ is conserved, show that $\frac{d}{dt}\|\Pi\|^2 = 0$.

$$\|\Pi\|^2 = \Pi \cdot \Pi$$

$$\frac{d}{dt}\|\Pi\|^2 = \dot{\Pi} \cdot \Pi + \Pi \cdot \dot{\Pi}$$

$$\frac{d}{dt}\|\Pi\|^2 = 2\,\dot{\Pi} \cdot \Pi$$

$$\frac{d}{dt}\|\Pi\|^2 \stackrel{?}{=} 0$$

$$2\dot{\Pi}\cdot\Pi \stackrel{?}{=} 0$$

$$\dot{\Pi}\cdot\Pi \stackrel{?}{=} 0$$

$$[\Pi\times\Omega + \alpha\Pi\times(\Pi\times\Omega)]\cdot\Pi \stackrel{?}{=} 0$$

$$(\Pi\times\Omega)\perp\Pi$$

$$\Rightarrow (\Pi\times\Omega)\cdot\Pi = 0$$

$$\Pi\times(\Pi\times\Omega)\perp\Pi$$

$$\Rightarrow [\alpha\Pi\times(\Pi\times\Omega)]\cdot\Pi = 0$$

$$\frac{d}{dt}\|\Pi\|^2 = 2\dot{\Pi}\cdot\Pi = 2(0+0)$$

$$\frac{d}{dt}\|\Pi\|^2 = 0$$

16.3 Dissipation of Kinetic Energy for Nonprincipal Axis Rotations

$\bullet H \searrow$

To show $H \searrow$, show that $\frac{d}{dt}H < 0$.

$$\begin{aligned} H &= \frac{1}{2}(\Pi\cdot\Omega) \\ \frac{d}{dt}H &= \frac{d}{dt}\frac{1}{2}(\Pi\cdot\Omega) \\ &= \dot{\Pi}\cdot\Omega \\ &= \alpha[\Pi\times(\Pi\times\Omega)]\cdot\Omega \\ &= \alpha[(\Omega\times\Pi)\cdot(\Pi\times\Omega)] \\ &= -\alpha||\Pi\times\Omega|| \end{aligned}$$

$||\Pi\times\Omega|| = 0$ for principal axis rotations. In this case $\frac{d}{dt}H = 0$, which is desired.

For non-principal axis rotations $||\Pi\times\Omega|| > 0$ and kinetic energy is dissipated, again as is desired.

16.4 Direction of the Angular Momentum Vector in Inertial Space

The direction of the angular momentum vector in inertial space π, is not preserved by the Marsden energy sink as $\dot{\pi} \neq 0$.

$$\begin{aligned}
\pi &= R\Pi \\
\dot{\pi} &= \dot{R}\Pi + R\dot{\Pi} \\
&= -R(\Pi \times \Omega) + R[(\Pi \times \Omega) + \Pi \times (\Pi \times \Omega)] \\
&= -R(\Pi \times \Omega) + R(\Pi \times \Omega) + R\Pi \times (\Pi \times \Omega)] \\
\dot{\pi} &= R\Pi \times (\Pi \times \Omega) \\
\dot{\pi} &= \pi \times (\Pi \times \Omega)
\end{aligned}$$

The angular momentum vector only remains fixed in inertial space for rotations about principal axes. Otherwise, it appears to move in inertial space. It is interesting to note that the angular momentum vector remains fixed in inertial space only for motions which *do not* dissipate kinetic energy.

16.5 Trajectories on the Momentum Sphere with Marsden Energy Sink

The trajectories of the tip of the angular momentum vector on the angular momentum sphere for

$$\dot{\Pi} = \Pi \times \Omega \; + \; \alpha\, \Pi \times (\Pi \times \Omega)$$

are qualitatively hand drawn in Figure 5.

17 Comparison of the Marsden and [Kammer and Gray 92] Energy Sinks

17.1 [Kammer and Gray 92] Energy Sink

The [Kammer and Gray 92] energy sink added to the equations of motion of a rigid body result in

$$\begin{bmatrix} \dot{\Pi}_1 \\ \dot{\Pi}_2 \\ \dot{\Pi}_3 \end{bmatrix} = \begin{bmatrix} A_1 \cdot \Pi_2 \Pi_3 \\ A_2 \cdot \Pi_1 \Pi_3 \\ A_3 \cdot \Pi_1 \Pi_2 \end{bmatrix} + \begin{bmatrix} u_1 \\ u_2 \\ u_3 \end{bmatrix}$$

where

$$\begin{bmatrix} u_1 \\ u_2 \\ u_3 \end{bmatrix} = \beta \begin{bmatrix} -\Pi_1 \Pi_2^2 \\ \Pi_1^2 \Pi_2 - \Pi_2 \Pi_3^2 \\ \Pi_2^2 \Pi_3 \end{bmatrix}$$

17.2 Comparison of Computational Terms

Both the Marsden and [Kammer and Gray 92] energy sinks are cubic in the components of the angular momentum vector.

The [Kammer and Gray 92] energy sink is not a special case of the Marsden energy sink.

The Marsden energy sink cannot simulate the [Kammer and Gray 92] energy sink.

Proof: In order for the $\dot{\Pi} = \Pi \times \Omega + \alpha \Pi \times (\Pi \times \Omega)$ energy sink to simulate the Kammer and Gray energy sink, we must have $\alpha = \beta$, $A_2 = 0$ which implies $I_3 = I_1$, and $A_1 = A_3 = -1$ which cannot be satisfied if $I_3 = I_1$.

17.3 Comparison of Momemtum Preservation

Like the energy sink given by Marsden, the [Kammer and Gray 92] energy sink preserves the magnitude of the angular momentum vector. (See [Kammer and Gray 92, pp 55-56, Eqns (1),(2) and (7)])

17.4 Comparison of Kinetic Energy Dissipation

The rate of dissipation of kinetic energy for the [Kammer and Gray 92] energy sink is given by

$$\frac{d}{dt}H = \beta \left[A_3 \cdot \Pi_1^2 \Pi_2^2 + A_1 \cdot \Pi_2^2 \Pi_3^2\right]$$

Kammer and Gray assume $I_1 < I_2 < I_3$, therefore A_1 and A_3 will be negative in the expression for $\dot{H}$. Hence, $\dot{H} < 0$ and kinetic energy is dissipated.

The expression for kinetic energy dissipation for the Marsden energy sink is given by

$$\frac{d}{dt}H = -\alpha ||\Pi \times \Omega||$$

or

$$\frac{d}{dt}H = -\alpha \left[A_3^2 \cdot \Pi_1^2 \Pi_2^2 + A_2^2 \cdot \Pi_1^2 \Pi_3^2 + A_1^2 \cdot \Pi_2^2 \Pi_3^2\right]$$

The Marsden energy sink dissipates kinetic energy regardless of the ordering of I_1, I_2 and I_3. In fact, in the axisymmetric case where two of the principal mass moments of inertia are equal, the Marsden energy sink will dissipate kinetic energy.

Kinetic energy will not be dissipated for all cases of axisymmetric bodies using the [Kammer and Gray 92] energy sink. If $I_2 = I_3$, where $I_2, I_3 > I_1$, and $\Pi_1(t = 0) = \Pi_3(t = 0)$, then $\frac{d}{dt}H(t = 0) = 0$ and H is preserved.

The Marsden energy sink will dissipate kinetic energy under more general principal moment of inertia restrictions than the [Kammer and Gray 92] energy sink. It can possibly be used in the dynamical analysis of axisymmetric spacecraft.

17.5 Comparison of Motion of Angular Momentum Vector in Inertial Space

Neither the Marsden nor the [Kammer and Gray 92] energy sink preserve the direction of the angular momentum vector in inertial space for non-principal axis rotations.

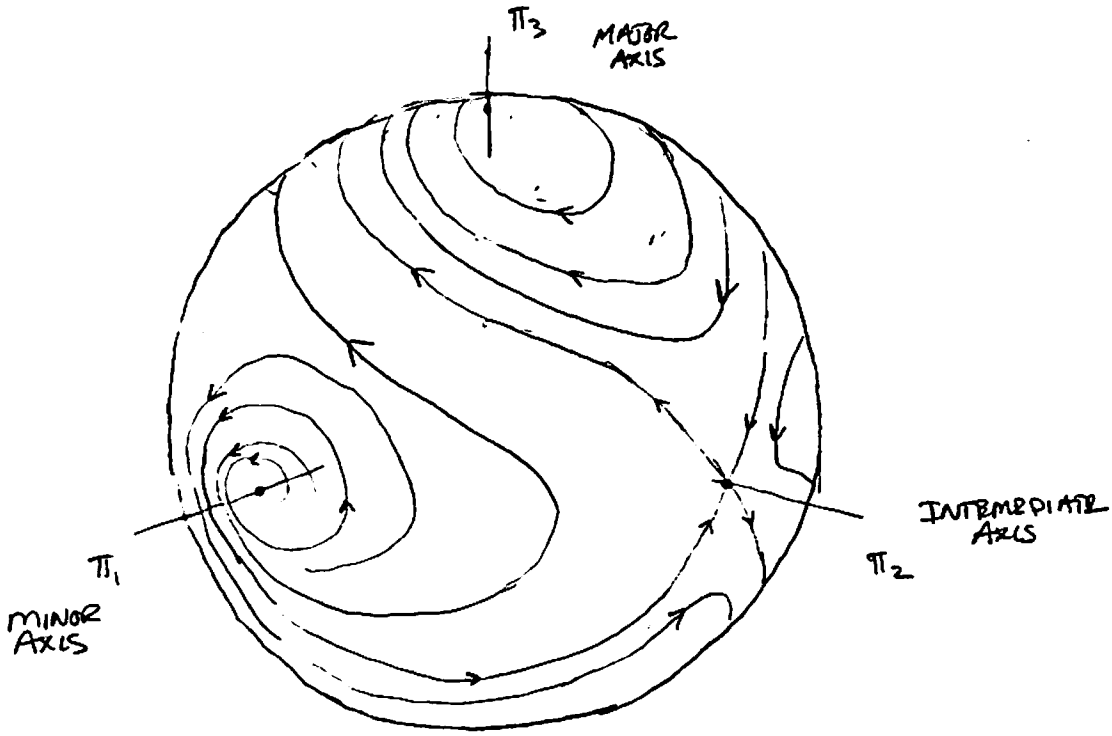

Figure 5: Angular Momentum Sphere Trajectories

References

[1] Mechanics

[Marsden and Ratiu 93] J. E. Marsden and T. S. Ratiu, em An Introductions to Mechanics and Symmetry, Vol 1, preprint.

[Hestenes 86] D. Hestenes. *New Foundations for Classical Mechanics.* D. Reidel Publishing Co, Dordrecht, Holland.

QA805.H581.1986 MATH

[2] Spacecraft Dynamics

[Agrawal 86] B. N. Agrawal, *Design of Geosynchronous Spacecraft.* Prentice-Hall, Englewood Cliffs, NJ, USA.

Dr Brig N. Agrawal is with the International Telecommunications Satellite Organization (INTELSAT), Washington, DC.

TK5104.A271.1986 ENGI

[Kane, Likins and Levinson 83] T. R. Kane, P. W. Likins, D. A. Levinson. *Spacecraft Dynamics.* McGraw-Hill, New York, NY, USA.

Prof Kane at Stanford is famous in the field and has been publishing since the 1950's. Prof Likins is also famous in field, is a contemporary of Kane and has been publishing in the field since the 1950's. Levinson is at Lockhed Palo Alto Research Laborartory.

TL1050.K36.1983 ENGI

[Pocha 87] J. J. Pocha. *An Introduction to Mission Design for Geostationary Satellites.* D. Reidel Publishing Co, Dordrecht, Holland.

TK5104.P6311.1987 ENGI

[Pritchard, Suyderhoud and Nelson 93] W. L. Pritchard, H. G. Suyderhoud, R. A. Nelson. *Satellite Communication Systems Engineering,* 2nd ed. Prentice-Hall, Englewood Cliffs, NJ, USA.

TK5104.P74.1993 ENGI

[Rimrott 89] F. P. J. Rimrott, *Introductory Attitude Dynamics.* Springer-Verlag, New York, 1989.

TL1050.R56.1989 ENGI

Rimrott is with the Dept of Mech Eng at the Univ of Toronto.

[Williamson 90] M. Williamson. *The Communications Satellite.* Adams Hilger, Bristol, England.

TK5104.W55.1990 ENGI

[3] Energy Sinks

[Kammer and Gray 92] D. C. Kammer and G. L. Gray, "A Nonlinear Control Design for Energy Sink Simulation inthe Euler-Poinsot Problem", *Journal of the Astronautical Sciences*, Vol 41, No 1, 1993, pp 53-72.

[4] Chaos in Spacecraft Dynamics

[Gray, Kammer and Dobson 93] G. L. Gray, D. C. Kammer and I. Dobson, "Chaos in an Attitude Maneuver of a Spacecraft Containing a Viscous Damper", Submitted to the *Jounal of Guidance, Control, and Dynamics Journal of Applied Mechanics.*

[Gray, Dobson and Kammer 92] G. L. Gray, I. Dobson and D. C. Kammer, "Chaos in a Spacecraft Passive Attitude Maneuver Due to Time-Periodic Perturbations", Submitted to the *ASME Journal of Applied Mechanics* on November 5, 1992.

Rigid single body spacecraft. Perturbed by small $\mathcal{O}(\epsilon)$ oscillating masses whose position is known as a function of time. Kinetic energy dissipation simulated by an energy sink method which reduced the KE while conserving (maintaining magnitude) of angular momentum vector. Melnikov integral, $M(t_o)$ calculated to show that under certain conditions, chaos is exhibited. This chaos is noted to be transient.